

# Online Research @ Cardiff

This is an Open Access document downloaded from ORCA, Cardiff University's institutional repository: <https://orca.cardiff.ac.uk/id/eprint/97716/>

This is the author's version of a work that was submitted to / accepted for publication.

Citation for final published version:

Harris, Kenneth David Maclean ORCID: <https://orcid.org/0000-0001-7855-8598> 2017. Explorations in the dynamics of crystalline solids and the evolution of crystal formation processes. Israel Journal of Chemistry 57 , pp. 154-170. 10.1002/ijch.201600088 file

Publishers page: <http://dx.doi.org/10.1002/ijch.201600088>  
<<http://dx.doi.org/10.1002/ijch.201600088>>

Please note:

Changes made as a result of publishing processes such as copy-editing, formatting and page numbers may not be reflected in this version. For the definitive version of this publication, please refer to the published source. You are advised to consult the publisher's version if you wish to cite this paper.

This version is being made available in accordance with publisher policies.

See

<http://orca.cf.ac.uk/policies.html> for usage policies. Copyright and moral rights for publications made available in ORCA are retained by the copyright holders.



# Explorations in the Dynamics of Crystalline Solids and the Evolution of Crystal Formation Processes

Kenneth D. M. Harris\*[a]

In honour of Professor Jack D. Dunitz FRS, on the 60th anniversary of establishing his research group at ETH, Zürich

**Abstract:** This article describes a few selected areas of (ammonium cyanate) that is not amenable to structural research within the field of structural chemistry, with characterization by single-crystal X-ray diffraction is also emphasis on aspects that have been influenced and inspired presented. On the theme of exploring the time evolution of by the seminal work of Jack Dunitz. The topics covered crystallization pathways, the recent development and application of in situ solid-state NMR techniques for mapping time-dependent changes that occur in the solid phase during include the study of dynamic properties of crystalline materials, focusing on the use of solid-state  $^2\text{H}$  NMR spectroscopy to unravel details of dynamic hydrogen-bonding crystallization processes are discussed. Finally, the article arrangements in crystalline alcohols and amino acids, as well as the use of in situ Raman microspectrometry to physicochemical understanding of crystal nucleation explore molecular transport processes through porous crystals. A case study involving the determination of both challenge in structural chemistry in the next few decades. structural properties and dynamic properties of a material

**Keywords:** crystal growth · Jack Dunitz · structural chemistry · dynamics of solids

## 1. Introduction

Although I had listened to many inspiring lectures by Jack Dunitz at conferences and had read several of his seminal publications, my first meeting with this great scientist was actually at an interview. In 1995, I had been encouraged to apply for the Chair of Structural Chemistry at the University of Birmingham, and one of the two external assessors for the appointment was Jack Dunitz. The interview process spanned two days. Jack was present on both days, so there was plenty of opportunity to enjoy talking about science with him, as well as facing his questions at the interview!

After moving to Birmingham, the next time I met Jack was at the ICCOSS meeting at Stony Brook, USA in 1997. While chatting to him after the conference dinner, he suggested that we should collaborate to determine the crystal structure of ammonium cyanate. Amazingly, in spite of the historical significance of this material, the crystal structure had never been previously reported. The problem was that single crystals of ammonium cyanate are impossible to prepare, so the only opportunity to determine the crystal structure would be to use powder diffraction data. Fortunately, my group was developing new techniques to determine the structures of organic materials from powder diffraction data (the subject of my lecture at Stony Brook), and Jack had clearly identified the opportunity to utilize our powder diffraction techniques to solve this long-standing, unresolved problem in structural chemistry. As an aside, one of Jack's remarkable characteristics, which I have come to realize over the years, is his

colossal knowledge of the literature, and his ability to make direct and meaningful connections between topical issues of the present day and work published in the long and distant past.

Although our first meeting took place as described above, my first "interaction" with the science of Jack Dunitz occurred much earlier. During my Ph.D. research in organic solid-state chemistry at the University of Cambridge, my supervisor (Sir John Meurig Thomas FRS) encouraged me to read the literature widely, and in particular, he pointed my reading in the direction of the work of Jack Dunitz. In addition to his seminal book,<sup>[1]</sup> *X-ray Analysis and the Structure of Organic Molecules*, which was probably the most influential book in my process of learning the foundations of X-ray diffraction, I became very interested in the papers that he was publishing around that time<sup>[2–4]</sup> on the physical interpretation of atomic displacement parameters (as determined in structure refinement from single-crystal X-ray diffraction data), especially as he was exploiting this information in imaginative ways to deduce insights into the dynamics of crystals. His 1988 paper<sup>[3]</sup>

---

[a] K. D. M. Harris  
School of Chemistry  
Cardiff University  
Park Place  
Cardiff CF10 3AT (Wales) E-mail:  
HarrisKDM@cardiff.ac.uk

with Schomaker and Trueblood in the *Journal of Physical Chemistry* particularly captivated my scientific imagination. It begins with the following sentences:

“The idea that atoms and molecules move in crystals – indeed move sometimes with large amplitude – would have struck most chemists of earlier generations as outlandish. Professor Leopold Ruzicka once opined (to one of us) that “a crystal is a chemical cemetery”. We know what he meant: long rows of molecules, interred in a rigid geometrical arrangement, lifeless compared with the molecular mazurkas that can be imagined to occur in solution. The view that Ruzicka expressed ... is perhaps still widely shared among chemists and even (we suspect) among some crystallographers. It should not be.”

These sentences seemed to convey so convincingly the necessity of giving due consideration to dynamic aspects of solids (and perhaps convey even more convincingly the folly of not doing so!). As in many other areas of structural chemistry, it was clear from this paper, and his other publications on similar topics, that Jack was striving to achieve a much deeper physical understanding of the values of atomic displacement parameters, when it seemed that many other crystallographers were content instead to regard atomic displacement parameters simply as a convenient means of absorbing multiple errors in their refinements. Indeed, as illustrated by this example, Jack always seems to be thinking more deeply than others across the field of structural chemistry, especially as his thinking is very firmly rooted in a profound understanding of thermodynamics and other aspects of physical chemistry.

Clearly, diffraction techniques have provided so much information that has enriched our understanding of structure across the full range of chemical, physical, biological, geological and materials sciences, but yet diffraction provides just the time-averaged picture of a crystal. To search beyond this time-averaged picture, we need to encompass other experimental and computational techniques which reveal the time dependence of structural properties across a range of different timescales. Motivated by this quest, my group has been interested over many years in exploring dynamic properties of solids, especially using solid-state NMR spectroscopy, but also

incoherent quasi-elastic neutron scattering (IQNS) and molecular dynamics simulations. Although such techniques reach beyond the time-averaged description provided by diffraction techniques, it is critical to recall that results from diffraction experiments provide an essential constraint in the interpretation of data from these techniques, as the time average of the correct dynamic model must agree with the time-averaged structural description obtained from diffraction data.

As an illustration of some of the dynamic processes that can occur in organic solids, Section 2 describes a few examples of dynamic hydrogen-bonding arrangements that we have explored using solid-state NMR techniques, and studies of molecular translation through porous crystals studied by in situ confocal Raman microspectrometry.

In Section 3, I return to consider the ammonium cyanate system, covering both the crystal structure of this material (Figure 1) determined from powder X-ray and neutron diffraction data, the focus of our collaboration with Jack Dunitz, and a subsequent investigation of the dynamic properties of this material.

Another aspect of crystalline materials that is critically important in both fundamental and applied contexts is to understand the fundamental processes underlying the formation and growth of crystals. In my opinion, the most significant challenge in structural chemistry in the next few decades will be to derive a fundamental physicochemical understanding of the process of crystal nucleation (see Section 5), and then to devise strategies to exploit this understanding to enable crystallization processes to be controlled such that they are directed towards very specific desired outcomes.

On a related theme of exploring the evolution of crystallization pathways, much of our recent research has been focused on the development and application of in situ solid-state NMR techniques for mapping the time-dependent changes that occur in the solid phase during crystallization (for example, to identify the polymorphic form<sup>[5–7]</sup> of the solid phase present as a function of time, and to monitor the structural evolution of the solid phase), as well as to unravel the corresponding changes that occur in the liquid phase. Although our experimental strategy is only able to explore the



Kenneth D.M. Harris graduated with a BSc degree in Chemistry from the University of St. Andrews (Scotland) in 1985, and then received a stimulating education in Solid-State Chemistry by carrying out research for his PhD degree under the supervision of Professor Sir John Meurig Thomas FRS at the University of Cambridge and at the Royal Institution, London between 1985 and 1988. After completing the PhD degree, he held positions as Lecturer in Physical Chemistry at the University of St. Andrews and then at University College London. He was appointed as Professor of Structural Chemistry at the University of Birmingham in 1995, and took up his present appointment as Distinguished Research Professor at Cardiff University in 2003. He has been awarded the Meldola (1991), Marlow (1996), Corday-Morgan (1999), Structural Chemistry (2001) and Tilden (2007/8) Medals of the Royal Society of Chemistry, and has been elected as a Fellow of the Royal Society of Edinburgh (2008), Fellow of the Learned Society of Wales (2011) and Member of Academia Europaea (2013). His research in the Physical Chemistry of Solids is focused on understanding fundamental aspects of the structural and dynamic properties of solids, and the development of experimental techniques for investigating these properties (particularly with regard to powder X-ray diffraction, solid-state NMR spectroscopy, and the new technique of X-ray Birefringence Imaging). He has held several appointments as Visiting Professor in Japan, France, U.S.A., Spain and Taiwan.



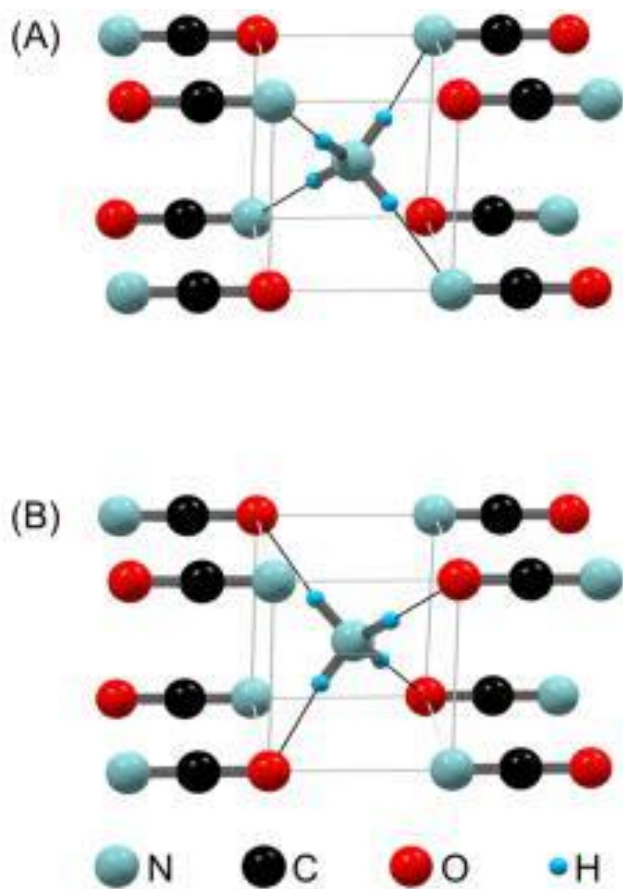


**Figure 1.** The crystal structure of ammonium cyanate. Two possible hydrogen-bonding arrangements are shown: (A) with the ammonium cation forming four N H...N hydrogen bonds; and (B) with the ammonium cation forming four N H...O hydrogen bonds. Powder neutron diffraction indicates that only hydrogen-bonding arrangement (A) exists in the crystal structure. Hydrogen bonds are shown as thin black lines.

crystallizing phase after the critical nucleation event has taken place, the technique can nevertheless yield significant insights into the sequence of events that occur at later stages along the crystallization pathway. Our recent work on the development and application of techniques in this field is summarized in Section 4.

Other aspects of the current research of my group, in particular our on-going development and application of techniques for structure determination of organic materials from powder X-ray diffraction data<sup>[8]</sup> and our development of the new technique of X-ray birefringence imaging,<sup>[9]</sup> are discussed in another article<sup>[10]</sup> within this special issue.

## 2. Dynamic Properties of Crystalline Solids

### 2.1 Introduction

As conveyed so eloquently in the quotation of Jack Dunitz<sup>[3]</sup> in Section 1, there is an unfortunate tendency (even among structural chemists) to regard crystalline solids as rigid assemblies of atoms or molecules, completely devoid of the interesting dynamic processes that occur for the same molecules and atoms when the solid is transformed into the molten or gaseous state, or when the crystalline solid is dissolved in solution. Conventional crystallographic models, so useful for displaying the fascinating arrangements of molecules and atoms in crystal structures, tend to convey the impression that the molecules and atoms are fixed rigidly in place, each constrained to reside motionlessly in its assigned position within the architecture of the crystal. But the molecules and atoms in a crystalline solid are certainly not motionless – they are dynamic entities, whether through small amplitude vibrational motions about their equilibrium positions or, in some cases, through large-scale reorientational motions, chemical exchange processes, or diffusion of molecules through crystals. Clearly, the occurrence of dynamic processes may have a significant influence on the physical properties of crystalline materials (including properties that may underpin materials applications, such as optical, electrical and magnetic properties). Thus, to derive a fundamental understanding of the properties of a material, it is essential not only to consider the time-averaged crystal structure, as revealed by diffraction-based techniques, but also to consider the time dependence of the crystal structure, as described by the variety of dynamic processes that can occur across a range of timescales.

Several experimental and computational techniques, including solid-state NMR spectroscopy, incoherent quasielastic neutron scattering, molecular dynamics simulation, Raman scattering, Brillouin scattering, and dielectric relaxation can probe the dynamic properties of solids, with each technique appropriate for studying dynamic processes occurring on a particular characteristic timescale. Among these techniques, solid-state NMR<sup>[11, 12]</sup> is particularly powerful, since by judicious choice of the specific NMR-active nucleus and the specific NMR phenomenon to be investigated, detailed information on a wide range of different types of dynamic process, occurring over a wide range of timescales, can be established. These dynamic processes include intramolecular dynamics (such as interconversion of a molecule between different conformations, rotation about bonds, and dynamic tautomerism), as well as reorientational motions of the whole molecule (as observed for guest molecules in solid inclusion compounds and for molecules in other rotator phase solids). In many cases, more than one type of dynamic process may occur in the material, often at different rates, and each process may be studied selectively by appropriate choice of NMR techniques. This section gives a few illustrative examples of some types of dynamic process that can occur in crystalline organic solids,

highlighting the application of solid-state NMR techniques (particularly broad-line  $^2\text{H}$  NMR) to probe these processes.

## 2.2 Dynamics of Hydrogen-Bonding Arrangements Revealed by Solid-state $^2\text{H}$ NMR Spectroscopy

### 2.2.1 Brief Background to Solid-state $^2\text{H}$ NMR

Solid-state  $^2\text{H}$  NMR is a powerful technique for studying reorientational motions of molecules in solids,<sup>[12–17]</sup> and has been used to characterize the dynamic properties of a wide range of systems. Different aspects of solid-state  $^2\text{H}$  NMR yield different information on dynamic properties, and the two most commonly used techniques are  $^2\text{H}$  NMR line-shape analysis and  $^2\text{H}$  NMR spin-lattice relaxation time measurements.

For  $^2\text{H}$  nuclei in organic solids, the quadrupolar interaction is normally so large that other nuclear spin interactions are negligible in comparison. A polycrystalline powder sample containing a random distribution of crystal orientations gives a characteristic  $^2\text{H}$  NMR “powder pattern” (several examples of which are shown in figures below). Analysis of the  $^2\text{H}$  NMR powder pattern allows quantitative determination of the quadrupole interaction parameters (the quadrupole coupling constant  $c$  and the asymmetry parameter  $\eta$ ) for the  $^2\text{H}$  nucleus. As the quadrupole interaction parameters are influenced significantly when the  $^2\text{H}$  nucleus undergoes motion on an appropriate timescale (see below), the appearance of the  $^2\text{H}$  NMR powder pattern changes significantly, depending on the rate and mechanism of the motion. When the  $^2\text{H}$  nucleus is static, or undergoes rates of motion lower than ca.  $10^3 \text{ s}^{-1}$  (the static/slow motion regime), the  $^2\text{H}$  NMR line shape has a

characteristic shape that is independent of the rate and geometry of the motion.  $^2\text{H}$  NMR line-shape analysis is particularly informative when the rate of motion is in the range  $10^3 \text{ s}^{-1}$  to  $10^8 \text{ s}^{-1}$  (the intermediate motion regime), as analysis of the  $^2\text{H}$  NMR line shape in this regime provides detailed information on the rate and mechanism of the dynamic process. For rates of motion higher than ca.  $10^8 \text{ s}^{-1}$  (the rapid motion regime), the actual rate of motion cannot be established from  $^2\text{H}$  NMR line-shape analysis, but information on the geometry and mechanism of the motion can still be obtained.  $^2\text{H}$  NMR line-shape analysis is generally carried out by calculating the line shapes for proposed dynamic models, and finding the dynamic model for which the set of calculated line shapes give rise to the best fit to the set of experimental line shapes recorded as a function of temperature. When the rate of motion is in the rapid regime with respect to  $^2\text{H}$  NMR line-shape analysis, detailed dynamic information may also be obtained from measurement and analysis of the  $^2\text{H}$  NMR spin-lattice relaxation time ( $T_1$ ), which is particularly sensitive for studying dynamic processes with rates in the range  $10^3$  to  $10^8 \text{ s}^{-1}$  (where  $\omega$  is the  $^2\text{H}$  Larmor frequency).

Solid-state  $^2\text{H}$  NMR has been used widely to study molecular dynamics in materials, including dynamics of rotator phase solids (plastic crystals), the dynamics of guest molecules in crystalline inclusion environments, reorientational motions of individual functional groups, and the motional properties of polymers and membranes.

### 2.2.2 Hydrogen-Bond Dynamics in Crystalline Amino Acids

Crystalline forms of the proteinogenic amino acids have often been used as model compounds for probing functional group interactions in proteins. In the crystalline state, the amino acids exist (in general) in the zwitterionic form  $[\text{RR}'\text{C}(\text{NH}_3^+)(\text{CO}_2^-)]$ , and the ammonium ( $\text{NH}_3^+$ ) group is often engaged in three intermolecular  $\text{N}-\text{H}\cdots\text{O}$  hydrogen bonds. In such cases, the crystal structures established from X-ray diffraction look perfectly ordered in every aspect, and the possibility that the  $\text{C}-\text{NH}_3^+$  group may actually undergo a 3-site 120° jump motion about the  $\text{C}-\text{N}$  bond is “hidden” from the diffraction data because the local symmetry of the dynamic process matches the local symmetry of the dynamic moiety (in this case, local 3-fold symmetry). We note that a 3-site 120° jump motion implies that the  $\text{C}-\text{NH}_3^+$  group has a specific residence time ( $\tau$ ) in a particular orientation, followed by an essentially instantaneous jump (by 120° rotation about the  $\text{C}-\text{N}$  bond) to an identical orientation, and so on. The time average over this jump motion (for which the rotation frequency is  $\nu = (3\tau)^{-1}$ ) is identical to the static situation, and the crystal structure determined from diffraction data reveals no evidence for the existence of any disorder.

Similarly, the crystal structure of urea determined from diffraction data<sup>[18–20]</sup> looks completely ordered, and does not reveal the fact that the urea molecule actually undergoes a 2-site 180° jump motion about the  $\text{C}=\text{O}$  bond axis (with the 2-fold symmetry of the jump process matching the 2-fold symmetry of the urea molecule).<sup>[21–24]</sup> Again, solid-state  $^2\text{H}$  NMR was a powerful technique for establishing the occurrence of the dynamic process in this case.

Focusing on crystalline amino acids, solid-state  $^2\text{H}$  NMR techniques have been applied<sup>[25]</sup> to establish the dynamics of ammonium group reorientation in samples of the  $\alpha$  polymorph and  $\beta$  polymorph of L-glutamic acid  $[\text{HO}_2\text{CCH}_2\text{CH}_2\text{CH}(\text{NH}_3^+)(\text{CO}_2^-)]$  deuterated in the ammonium group (i. e.,  $\text{ND}_3^+$ ). The fact that the solid-state  $^2\text{H}$  NMR spectrum of each polymorph changes significantly as a function of temperature (see Figure 2 and Figure 3) reveals clearly that the  $\text{C}-\text{ND}_3^+$  groups are dynamic. In the crystal structure of each polymorph, determined from single-crystal neutron diffraction data,<sup>[26, 27]</sup> the  $\text{C}-\text{ND}_3^+$  group forms three intermolecular  $\text{N}-\text{D}\cdots\text{O}$  hydrogen bonds. The changes in the experimental  $^2\text{H}$  NMR spectra as a function of temperature are completely described by the 3-site 120° jump model discussed above. From the best-fit simulated  $^2\text{H}$  NMR spectrum corresponding to each experimental  $^2\text{H}$  NMR spectrum, the rate ( $k$ ) of the 3-

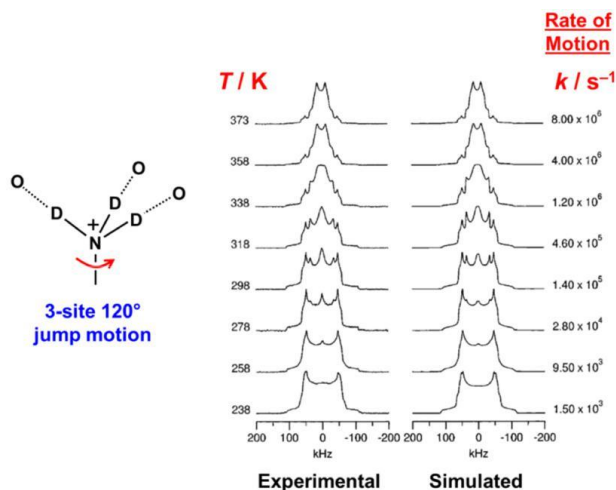


**Figure 2.** Experimental solid-state  $^2\text{H}$  NMR spectra recorded as a function of temperature for a powder sample of the a polymorph of deuterated L-glutamic acid, and the best-fit simulated solid-state  $^2\text{H}$  NMR spectrum at each temperature, calculated for the dynamic model (3-site 1208 jump motion of the  $\text{ND}_3^+$  group). A schematic of the dynamic model is shown at the left.

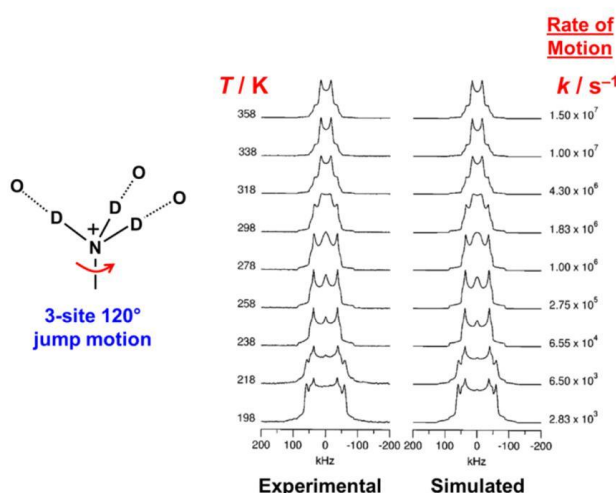


**Figure 3.** Experimental solid-state  $^2\text{H}$  NMR spectra recorded as a function of temperature for a powder sample of the b polymorph of deuterated L-glutamic acid, and the best-fit simulated solid-state  $^2\text{H}$  NMR spectrum at each temperature, calculated for the dynamic model (3-site 1208 jump motion of the  $\text{ND}_3^+$  group). A schematic of the dynamic model is shown at the left.

site 1208 jump motion is established at each temperature studied (see Figures 2 and 3).

From Figures 2 and 3, it is clear that there are significant differences in the rate of the  $\text{ND}_3^+$  group reorientation (at a given temperature) in the two polymorphs. On the assumption of Arrhenius behaviour for the temperature dependence of the rate of reorientation of the  $\text{ND}_3^+$  group (Figure 4), the activation energy for this motion was determined to be (47

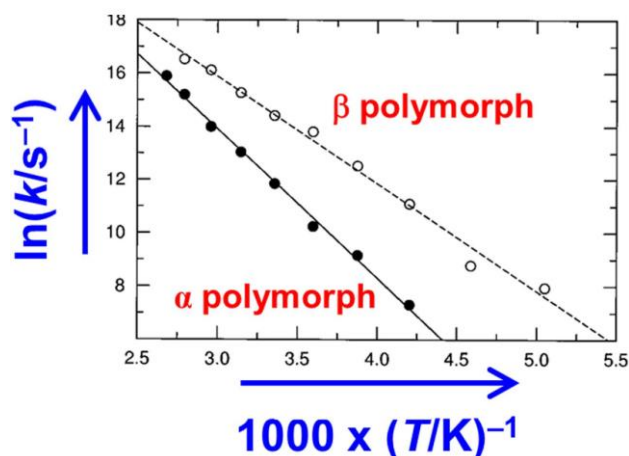


**Figure 4.** Arrhenius plots for the 3-site 1208 jump motion of the  $\text{ND}_3^+$  group in the a polymorph (filled circles) and b polymorph (open circles) of deuterated L-glutamic acid, determined from best-fit simulations of the  $^2\text{H}$  NMR line shapes shown in Figures 2 and 3. The straight lines are linear least-squares fits.

2)  $\text{kJ mol}^{-1}$  for the a polymorph and (34 ± 3)  $\text{kJ mol}^{-1}$  for the b polymorph, in good agreement with results from  $^1\text{H}$  NMR spin-lattice relaxation time data, from which the activation energy was established to be (48 ± 1)  $\text{kJ mol}^{-1}$  for the a polymorph and (39 ± 2)  $\text{kJ mol}^{-1}$  for the b polymorph. In the crystal structures of the a and b polymorphs,<sup>[26, 27]</sup> there are only small differences in the distances and angles that define the hydrogen-bond geometries in the two polymorphs. However, these small differences in hydrogen-bonding geometries involving the  $\text{ND}_3^+$  group suggest that the hydrogen bonding is stronger in the a polymorph, consistent with the observation from our  $^2\text{H}$  NMR study that the activation energy for the ammonium group reorientation is higher for the a polymorph.

Another interesting issue for proteinogenic amino acids is to compare the properties of racemic and enantiomerically pure crystalline forms.<sup>[28]</sup> With regard to dynamic properties, solid-state  $^2\text{H}$  NMR studies have been carried out<sup>[29]</sup> on the racemic and enantiomerically pure crystalline forms of serine [ $\text{HOCH}_2\text{CH}(\text{NH}_3^+)(\text{CO}_2^-)$ ], for samples of DL-serine and L-serine deuterated in the ammonium group. For both L-serine and DL-serine,  $^2\text{H}$  NMR line-shape analysis indicates that the  $\text{ND}_3^+$  group undergoes a 3-site 1208 jump motion. At a given temperature, the jump frequency ( $k$ ) is substantially higher for L-serine (for example, at 233 K,  $k = 5.0 \pm 10^6 \text{ s}^{-1}$  for L-serine and  $k = 6.0 \pm 10^4 \text{ s}^{-1}$  for DL-serine). The results from both  $^2\text{H}$  NMR line-shape analysis (LA) and  $^2\text{H}$  NMR spin-lattice relaxation time measurements (SLR) indicate that the

activation energy for the 3-site 1208 jump motion of the  $\text{ND}_3^+$  group is significantly higher for DL-serine (38.0  $\text{kJ mol}^{-1}$  (LA); 39.7 ± 0.81  $\text{kJ mol}^{-1}$  (SLR)) than for L-serine (23.4 ± 0.8  $\text{kJ mol}^{-1}$  (LA); 23.8 ± 0.3  $\text{kJ mol}^{-1}$  (SLR)), suggesting that the hydrogen bonding involving the  $\text{ND}_3^+$  group may be significantly stronger in the case of the racemic material.

The effects of hydrogen bonding on ammonium group dynamics have also been studied in several other crystalline amino acids.<sup>[30–32]</sup>

It is relevant to ponder the extent to which these significant differences in rotational frequencies of functional groups may contribute to differences in the entropies of the different crystal forms under comparison, and hence may contribute to differences in their Gibbs energies. Given the considerable current interest (see Section 5) in computational studies to assess the relative energies of different solid forms of materials (e. g., different polymorphs, or racemic versus enantiomerically pure forms), it is important to consider whether differences in rotational dynamics of functional groups may influence the ranking of structures based on Gibbs energies. Given that the existence of certain motions (such as the 3-site 1208 jump motion of ammonium groups in amino acids) is not even revealed by diffraction techniques, and to establish the rates of such motions requires detailed spectro-

scopic studies (such as the <sup>2</sup>H NMR studies described above), it is clear that standard computational approaches to assess energetic properties of crystalline solids based purely on consideration of time-averaged crystal structures may be missing certain factors that could have an important influence on the relative energetic ordering of different crystalline forms.

### 2.2.3 Hydrogen-Bond Switching in Crystalline Alcohols

In the crystal structure of triphenylmethanol (Ph<sub>3</sub>COH),<sup>[33]</sup> the molecules form hydrogen-bonded “tetramers”, with the oxygen atoms positioned approximately at the corners of a tetrahedron (Figure 5). The point symmetry of the tetramer is C<sub>3</sub> (rather than T<sub>d</sub>); thus, three Ph<sub>3</sub>COH molecules (denoted “basal”) are related to each other by a 3-fold rotation axis, and the other molecule (denoted “apical”) lies on this axis. Thus, the oxygen atoms from the four molecules in the tetramer form a pyramidal arrangement with an equilateral triangular base, and the O···O distances (ca. 2.9 Å) are consistent with the tetramer being held together by O H···O hydrogen bonds. As there are six O···O edges of the tetramer but only four O H···O hydrogen bonds, there are several different permutations for arranging the O H···O hydrogen bonds, and disorder of the hydrogen-bonding arrangement may be anticipated, consistent with the fact that hydrogen-atom positions were not reported for the hydroxyl groups in the crystal structure

determined from single-crystal X-ray diffraction data at ambient temperature. To explore whether the disorder of the hydrogen-bonding arrangement is dynamic, solid-state <sup>2</sup>H NMR studies were carried out<sup>[34]</sup> on the selectively deuterated material Ph<sub>3</sub>COD.

The solid-state <sup>2</sup>H NMR line shape for Ph<sub>3</sub>COD varies significantly as a function of temperature,<sup>[34]</sup> indicating that the hydrogen-bonding arrangement is dynamic. Several plausible dynamic models were considered, and it was found that only one model gives a good fit to the experimental solid-state

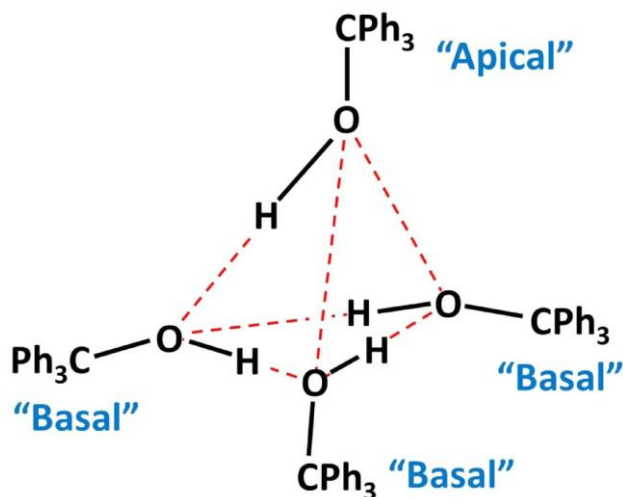


**Figure 5.** Schematic representation of the hydrogen-bonded “tetramer” in the crystal structure of triphenylmethanol. The hydrogen-bonding arrangement shown is only one of several possible hydrogen-bonding arrangements for the tetramer. The unique “apical” molecule and the three “basal” molecules are discussed in the text in the context of the dynamic model for hydrogen-bond switching.

<sup>2</sup>H NMR spectra across the full temperature range studied. In this model, the deuteron of the apical molecule undergoes a 3-site 1208 jump motion by rotation about the C O bond, with equal populations of the three sites, whereas the deuterons of the three basal molecules undergo 2-site 1208 jumps, by rotation about their C O bonds. In addition, each deuteron undergoes rapid libration about the relevant C O bond, with the libration amplitude increasing as a function of temperature. The behaviour of the basal molecules is interpreted in terms of the existence of two possible hydrogen-bonding arrangements (clockwise and anticlockwise) on the basal plane of the pyramid. The 2-site 1208 jump motion for the basal molecules “switches” between these two hydrogen-bonding arrangements, requiring correlated jumps of the hydroxyl groups of all three basal molecules. On the assumption of Arrhenius behaviour for the temperature dependence of the jump frequencies, the activation energies for the jump motions were determined to be 10 kJ mol<sup>−1</sup> for the apical deuteron and 21 kJ mol<sup>−1</sup> for the basal deuterons. This dynamic model is further supported by consideration of <sup>2</sup>H NMR spin-lattice relaxation time data.

Subsequent studies included a detailed analysis of the disordered hydrogen-bonding arrangement in triphenylmethanol using single-crystal neutron diffraction<sup>[35]</sup> and an investigation of the contrasting hydrogen-bond dynamics in the silicon analogue triphenylsilanol using solid-state <sup>2</sup>H NMR.<sup>[36]</sup> A theoretical study of the pathways for hydrogen-bond switching in a geometrically similar model system, comprising a tetrahedral hydrogen-bonded arrangement of methanol molecules, has also been reported.<sup>[37]</sup>



## Molecular Transport Through Porous Organic 2.3 Crystals

Many types of solid inclusion compound (for example, zeolites, aluminophosphates, and metal-organic frameworks) have important applications in molecular separation processes, based on the fact that selective incorporation and exchange of guest molecules of differing size and shape can occur, while

retaining the integrity of the host structure. Transport processes of molecules through the systems of interconnected tunnels and cages in such materials have been widely studied, and can be a critical factor in developing successful applications of these materials. For example, in applications of zeolites based on catalytic transformations or separation processes, the rate of diffusion of guest molecules within the zeolitic host structure<sup>[38, 39]</sup> may have an important bearing on the overall rate of the process.

For solid organic inclusion compounds, on the other hand, there are relatively few examples in which the crystal integrity of the host structure is maintained when the guest molecules are lost from the inclusion compound, thus limiting the prospects for carrying out guest exchange processes that proceed via the “empty” host structure. Nevertheless, a process for achieving guest exchange in such cases, by a mechanism that does not proceed via the empty host tunnel structure, has been identified<sup>[40]</sup> and has been demonstrated in the case of urea inclusion compounds.

Urea inclusion compounds are an extensively studied family of solid organic inclusion compounds,<sup>[41–45]</sup> in which linear-chain guest molecules (based on a long n-alkane chain) are arranged along one-dimensional tunnels (diameter ca. 5.25 Å) that exist within the urea host structure, which is constructed from a helical hydrogen-bonded arrangement of urea molecules (Figure 6). The fact that the urea tunnel structure is stable only when it is filled with a dense packing of guest molecules imposes a limitation on the opportunity to

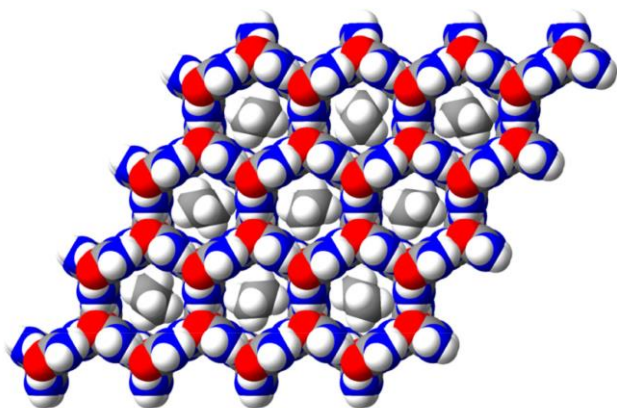


**Figure 6.** Crystal structure of the hexadecane/urea inclusion compound at ambient temperature, showing nine complete tunnels (with van der Waals radii) viewed along the tunnel axis. The hexadecane guest molecules have been inserted into the tunnels, illustrating orientational disorder.

develop potential applications based on molecular adsorption and/or molecular separation, analogous to the types of process that have been exploited for zeolitic host materials.

The proposed mechanism for guest exchange<sup>[40]</sup> (see Figure 7) is based on the requirement that the host tunnels remain fully occupied by guest molecules throughout the exchange process, but with the identity of the guest molecules changing as a function of time. The idea is that net transport of guest molecules in one direction along the host tunnel can be achieved by inserting “new” (thermodynamically more favourable) guest molecules at one end of a crystal of the inclusion compound (e. g., by dipping the crystal into the liquid phase of the new guest), with the “original” guest molecules expelled from the other end of the crystal.

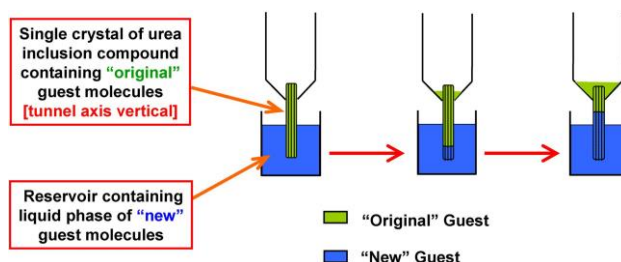


**Figure 7.** Mechanism for guest exchange in a single crystal of a urea inclusion compound. In the single crystal shown, the tunnels in the urea host structure are vertical.

The successful implementation of this guest exchange process has been demonstrated<sup>[40]</sup> in the case of urea inclusion compounds. To gain deeper insights into this process, confocal Raman microspectrometry has been exploited<sup>[46]</sup> as an in situ probe (Figure 8) to yield information on the spatial distribution of the original and new guest molecules within the crystal, and to establish how the spatial distribution of the original and new guest molecules changes as a function of time. The published work in this area has focused on using the 1,8-dibromooctane/urea inclusion compound as the “original”

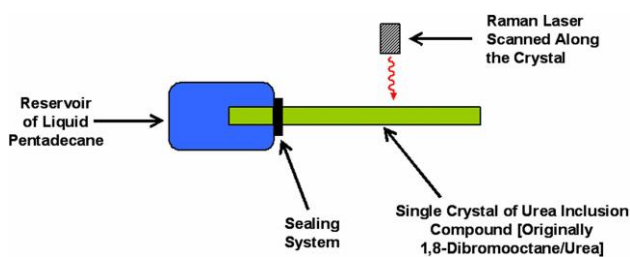


**Figure 8.** Schematic of the experimental assembly for in situ Raman microspectrometry studies of guest exchange in a urea inclusion compound, comprising the single crystal of the urea inclusion compound (green), initially containing 1,8-dibromooctane guest molecules, attached to a reservoir containing liquid pentadecane (blue).



crystal and pentadecane as the “new” type of guest molecule. For this system, analysis of the Raman microspectrometry data is based<sup>[46]</sup> on studying the variation of the intensity of the C Br stretching band of the original 1,8-dibromooctane guest molecules (for the predominant trans end-group conformation) as a function of position in the crystal and as a function of time (Figure 9). Such data provide quantitative information on kinetic and mechanistic aspects of the transport of guest molecules through the host tunnel structure during the guest exchange process,<sup>[47]</sup> revealing inter alia that unidirectional transport of guest molecules in this system occurs at a constant rate of ca.  $(70.3 \pm 2.2) \text{ nm s}^{-1}$  at ambient temperature. Furthermore, in situ studies using confocal Raman microspectrometry<sup>[48]</sup> have revealed that the guest exchange process is associated with significant changes in the conformational properties of the original (1,8-dibromooctane) guest molecules within the “boundary region” between the original and new guests, corresponding to a significant increase in the proportion of 1,8-dibromooctane guest molecules with the gauche end-group conformation. In addition, bi-directional transport of guest molecules through the urea tunnel structure has been demonstrated, and mechanistic details of this process have been rationalized.<sup>[49]</sup> At this stage, several fundamental aspects relating to such guest exchange processes remain to be understood; for example, studies to probe the temperature dependence of the rate of transport, and hence to establish activation parameters for the transport process, have not yet been reported. However, establishing an understanding of the fundamentals of guest exchange processes in such materials is a prerequisite for developing and optimizing a range of potential applications in molecular separation, based for example on discrimination of molecular size, shape, and chirality.

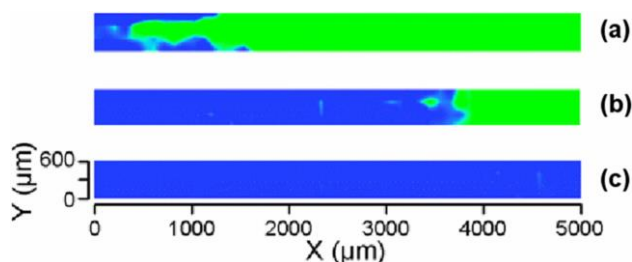


**Figure 9.** Results from time-resolved and spatially resolved monitoring of guest exchange in a single crystal of a urea inclusion compound using in situ Raman microspectrometry. The Raman micrographs were recorded during transport of pentadecane molecules into and along the tunnels, displacing the guest molecules (1,8-dibromooctane) originally present. The probed region shown represents only part of the crystal, and the transport of guest molecules occurs from left to right (the tunnels run horizontally in the micrographs shown). Regions coloured blue are rich in pentadecane and regions coloured green are rich in 1,8-dibromooctane. The time taken to record each micrograph was ca. 28 mins; the three micrographs shown were recorded: (a) 18 hrs; (b) 29 hrs; and (c) 40 hrs after commencing the guest exchange process.

### 3. Structure and Dynamics of Ammonium Cyanate: Collaboration with Jack Dunitz and Beyond

#### 3.1 Introduction

In 1828, Friedrich Woehler<sup>[50]</sup> observed, while attempting to prepare ammonium cyanate  $[\text{NH}_4^+ \text{OCN}^-]$  by a number of different routes, that urea  $[\text{O}=\text{C}(\text{NH}_2)_2]$  was formed instead. Subsequently, Woehler and Liebig<sup>[51]</sup> were successful in preparing solid ammonium cyanate, and demonstrated that, under appropriate conditions, this material undergoes a solid-state reaction to produce urea. These discoveries played a seminal role in the history of chemistry, as the reaction from ammonium cyanate to urea represented the first direct evidence that it is possible for an inorganic material to be converted into an organic substance that was known to occur in living systems. Subsequently, this reaction has received much attention, both in aqueous solution and in the solid state,<sup>[52]</sup> although most experimental studies have focused on the reaction in solution.

#### 3.2 Structural Properties

In spite of the importance of understanding structural properties of ammonium cyanate in the solid state, structure determination by single-crystal X-ray diffraction was precluded by the fact that this material can be prepared only as a microcrystalline powder.

Structure determination was carried out initially from powder X-ray diffraction data,<sup>[53]</sup> which established the positions of the non-hydrogen atoms, but could not reliably distinguish the orientation of the ammonium cation (as a consequence of the low X-ray scattering power of hydrogen). Subsequent powder neutron diffraction studies<sup>[54]</sup> were necessary to establish details of the hydrogen-bonding arrangement, as discussed below. The structure is tetragonal with space group  $P4/nmm$ . The nitrogen atom of the ammonium cation is located at the centre of a nearly cubic local arrangement of oxygen and nitrogen atoms (from cyanate anions), which occupy alternate corners of the “cube”. Two plausible orientations of the ammonium cation may be proposed, in one case forming four  $\text{N} \cdots \text{O}$  hydrogen bonds, and in the other case forming four  $\text{N} \cdots \text{N}$  hydrogen bonds (Figure 1). Powder neutron diffraction studies<sup>[54]</sup> on the deuterated material  $\text{ND}_4^+ \text{OCN}^-$  (actually with a percentage deuteration of ca. 77–81 %) definitively support the structure with  $\text{N} \cdots \text{N}$  hydrogen bonding, with no detectable extent of disorder between the  $\text{N} \cdots \text{O}$  and  $\text{N} \cdots \text{N}$  hydrogen-bonding arrangements. Thus, Rietveld refinement calculations for a structural model comprising both orientations of the ammonium cation with fractional occupancies  $x$  and  $(1-x)$ , respectively, converge towards a situation with zero occupancy of the deuterium nuclei in sites corresponding to  $\text{N} \cdots \text{O}$

hydrogen bonding and 100 % occupancy in sites corresponding to N D...N hydrogen bonding (across the temperature range from 14 K to 288 K investigated in the powder neutron diffraction study). Solid-state  $^{15}\text{N}$  NMR data<sup>[54]</sup> are also consistent with the existence of N H...N hydrogen bonding in this material.

### 3.3 Dynamic Properties

Although crystal structure determination from powder neutron diffraction data gives a well-defined, ordered, time-averaged structure, it is important to consider the possibility that dynamic processes may occur in this material. In the case of ammonium cyanate, it is also relevant to consider whether the onset of the solid-state chemical transformation to produce urea might be triggered by the occurrence of an appropriate dynamic process of the ammonium cation.

With these motivations, we carried out a comprehensive study of the dynamic properties of the ammonium cation in solid ammonium cyanate,<sup>[55]</sup> focusing on solid-state  $^2\text{H}$  NMR spectroscopy using the deuterated material (denoted  $\text{ND}_4^+ \text{OCN}^-$ ) and incoherent quasielastic neutron scattering (IQNS) using the material with natural isotopic abundances (denoted  $\text{NH}_4^+ \text{OCN}^-$ ). The combination of these two techniques is a powerful strategy for probing dynamic properties of organic materials, as together they allow molecular motions to be studied across a wide range of timescales. Relevant results from a computational study<sup>[56]</sup> of energy barriers for reorientation of the ammonium cation in ammonium cyanate are also important in the context of deriving dynamic models for this material.

A fundamental requirement of proposed models for dynamic processes in crystalline solids is that the time average of the dynamic process should be in agreement with the crystal structure determined from diffraction-based studies. As discussed above, powder neutron diffraction indicates that there is no observable population of hydrogen/deuterium sites corresponding to the orientation of the ammonium cation with N H...O hydrogen bonding. Thus, any dynamic model that implies a nonzero population of hydrogen/deuterium sites corresponding to N H...O hydrogen bonding would be incompatible with the experimental crystal structure. On this basis, the following models (which preserve only N H...N hydrogen bonds) were considered plausible.

**Model A:** 1808 jumps about one of the 2-fold axes of the ammonium cation in the crystal structure. Starting from the orientation with four N H...N hydrogen bonds, such jumps take the ammonium cation into an equivalent orientation with four N H...N hydrogen bonds.

**Model B:** 1208 jumps about one of the 3-fold axes of the ammonium cation in the crystal structure, with one N H bond (collinear with the rotation axis) remaining fixed during this motion.

**Model C:** A 4-site tetrahedral jump model, in which each hydrogen atom of the ammonium cation visits all four sites

(corresponding to the four N H...N hydrogen bonds) with equal probability during the timescale of the measurement. This situation could be achieved by individual jumps of the type discussed for model B (i. e., 3-site 1208 jumps about a single N H bond), but with the N H bond that serves as the rotation axis changing (on a time-dependent basis) such that each of the four N H bonds serves as the rotation axis with equal probability over the timescale of the measurement.

Solid-state  $^2\text{H}$  NMR spectra, recorded as a function of temperature for a powder sample of deuterated ammonium cyanate, are shown in Figure 10, together with the simulated  $^2\text{H}$  NMR line shapes for dynamic models A, B, and C. Visual comparison between experimental and simulated  $^2\text{H}$  NMR line shapes strongly favours the tetrahedral jump model for the dynamics of the ammonium cation (Model C). As discussed in Section 2, finding the simulated  $^2\text{H}$  NMR line shape that represents the best fit to the experimental  $^2\text{H}$  NMR line shape at each temperature allows the jump rate to be established as a function of temperature, thus allowing activation parameters to be assessed. However, the fact that the experimental  $^2\text{H}$  NMR line shape for ammonium cyanate is a single Gaussian line throughout most of the intermediate motion regime means that the fitting process to establish the jump rate that gives the best-fit line shape at each temperature is much less sensitive than usual. For this reason, analysis of  $^2\text{H}$  NMR spin-lattice relaxation time data provides a more reliable quantitative determination of activation parameters for the motion.

The temperature-dependence of the powder-average  $^2\text{H}$  NMR spin-lattice relaxation time  $\langle 1/T_1 \rangle_p$ , determined from 123 K to 290 K, is shown in Figure 11, together with a best-fit curve calculated for the tetrahedral jump model,<sup>[57]</sup>

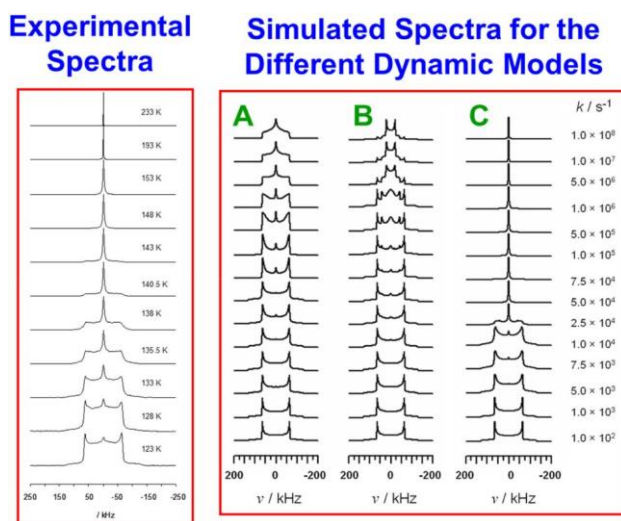


**Figure 10.** Left: Experimental solid-state  $^2\text{H}$  NMR spectra recorded as a function of temperature for a powder sample of deuterated ammonium cyanate. Right: Simulated solid-state  $^2\text{H}$  NMR spectra calculated for dynamic models A, B, and C defined in the text, for values of jump rate ( $k$ ) ranging from the slow/static motion regime to the rapid motion regime.

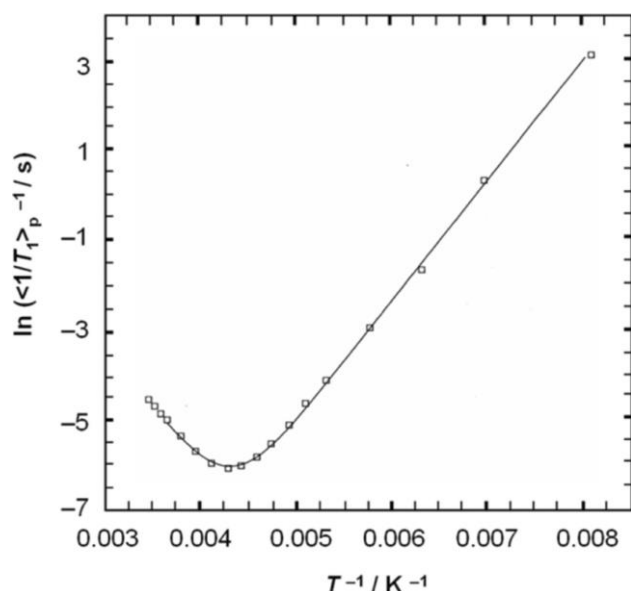


**Figure 11.** Temperature dependence of the powder-average  $^2\text{H}$  NMR spin-lattice relaxation time  $\langle 1/T_1 \rangle_p^{-1}$  for deuterated ammonium cyanate. The fitted line is the best fit to the experimental data using a theoretical expression for  $\langle 1/T_1 \rangle_p^{-1}$  based on the tetrahedral jump model (model C). From the fitting process, the activation energy for  $1.0$  kJ mol

under the assumption that the temperature dependence of the jump rate exhibits Arrhenius behaviour. The three fitted parameters in this expression are the static quadrupole coupling constant ( $c$ ), the activation energy ( $E_a$ ) and the pre-exponential factor ( $t_c^0$ ). The fitted theoretical expression is in excellent agreement with the experimental data, further supporting the tetrahedral jump model. The best-fit values of the activation parameters are:  $E_a = (21.9 \pm 1.0)$  kJ mol $^{-1}$  and  $\ln(t_c^0/s) = 31.3 \pm 0.8$ . These results are in good agreement (within experimental errors) with those determined from IQNS data

[ $E_a = (22.6 \pm 2.1)$  kJ mol $^{-1}$ ;  $\ln(t_c^0/s) = 30.6$ ], which also provides strong support for the tetrahedral jump model in ammonium cyanate. It is important to emphasize the advantages of the combined strategy of using solid-state  $^2\text{H}$  NMR spectroscopy and IQNS in the study of dynamic properties of organic solids, particularly as IQNS allows detailed characterization of motions that occur on shorter timescales than those that are accessible using solid-state  $^2\text{H}$  NMR techniques.

### 3.4 Comments on the Solid-state Reaction of Ammonium Cyanate to Urea

Although the crystal structure of ammonium cyanate is now known and the dynamic properties are understood, a comprehensive study of the solid-state chemical reaction from ammonium cyanate to urea has not yet been reported, although possible insights derived from computational studies have

been proposed.<sup>[58, 59]</sup> To address this issue, we are currently engaged in a detailed programme of research using a range of experimental techniques (including in situ powder X-ray diffraction and in situ solid-state NMR techniques) to gain a detailed understanding of kinetic and mechanistic aspects of this historically significant chemical reaction.

## 4. In Situ Solid-state NMR Strategies to Study the Evolution of Crystallization Processes

### 4.1 Introduction

Crystallization processes are encountered in many different scientific fields, and a deeper understanding of such processes has important practical implications, including the optimization of crystallization in industrial applications. Improving our fundamental mechanistic understanding relies on developing new experimental strategies, particularly those that allow direct in situ monitoring of the process.<sup>[60]</sup> Crystallization processes are generally governed by kinetic factors and metastable solid forms often crystallize initially (rather than the thermodynamically stable form). Subsequently, the crystallization may evolve through a sequence of different transient solid forms before the final product is obtained. To optimize and control crystallization processes, it is essential to understand the sequence of events that occur in the evolution of the solid phase, rather than simply characterizing the final product recovered at the end of the process. Exploiting experimental strategies that allow direct in situ monitoring is clearly essential in pursuit of this aim.

We have recently focused<sup>[61–66]</sup> on developing in situ solid-state NMR strategies for mapping the evolution of the solid phase during crystallization processes from solution. Here, we highlight the experimental method and present illustrative examples that reveal the types of information that can be obtained on the evolution of different solid forms (and interconversion between solid forms) during crystallization of organic systems from the solution state.

Importantly, the in situ solid-state NMR technique<sup>[61]</sup> exploits the ability of NMR to selectively detect the solid phase in the types of heterogeneous solid/liquid system that exist during crystallization from solution, with the liquid phase “invisible” to the measurement. This technique has been shown to be a powerful approach for establishing the sequence of solid phases produced during crystallization<sup>[62–64]</sup> and for the discovery of new (transient) solid forms.<sup>[65]</sup>

### 4.2 The In Situ Solid-state NMR Technique

Until recently, the prospect of using solid-state NMR for in situ studies of crystallization from solution was limited by the difficulty of securely sealing a liquid phase inside an NMR rotor such that fast magic-angle sample spinning (MAS),



which is required for recording high-resolution solid-state NMR spectra, can be carried out without problems arising from leakage of the liquid from the rotor. Recently, suitable rotor technology has been developed for sealing solutions inside NMR rotors for MAS experiments, greatly facilitating the development of the in situ solid-state NMR strategy described here.

In our in situ solid-state NMR strategy for monitoring crystallization (see Figure 12), a homogeneous (undersaturated) solution is initially prepared inside the NMR rotor at high temperature. Crystallization is induced by decreasing the temperature rapidly to a target temperature at which the solution is supersaturated, and hence crystallization is thermodynamically favoured. The time dependence of the crystallization process is then monitored by recording high-resolution solid-state NMR spectra repeatedly as a function of time. The time resolution of the in situ monitoring of the crystallization process is dictated by the time required to record an individual NMR spectrum of adequate quality to identify and distinguish the different solid forms present during the evolution of the system. Sufficiently good spectral resolution is also required to identify and assign the solid phases present at different stages of the crystallization process. Clearly, it is desirable to be able to detect and identify the first solid particles produced in the crystallization process, at which stage the amount of solid in the system is generally very low. Thus, optimization of the sensitivity of the measurement is also important, allowing solid-state NMR spectra of adequate quality to be recorded in the shortest possible time. To maximize the sensitivity, isotopic labelling of the material to be crystallized is desirable (although not always essential) and carrying out the experiments at high magnetic field is advantageous.

A crucial feature of the strategy is that, by appropriate choice of measurement conditions, solid-state NMR can give complete selectivity in detecting only the solid component in the system (and thus the dissolved solute and solvent are undetected in the measurement). For organic materials, such discrimination between solid and solution phases is readily achieved by recording  $^{13}\text{C}$  NMR spectra using the  $^1\text{H}/^{13}\text{C}$  cross-polarization (CP) technique. As a consequence of differences in dynamic behaviour between molecules in the solid

and solution states,  $^{13}\text{C}$  NMR spectra recorded using  $^1\text{H}/^{13}\text{C}$  CP contain signals only from the solid phase. Thus, even if only a small fraction of the solute has crystallized (e. g., in the early stages of crystallization), only the solid particles contribute to the measured NMR spectrum, and the dissolved solute (present in a much higher amount in the early stages of crystallization) and solvent are “invisible” to the measurement.

### 4.3 Example: Evolution of Different Solid Forms of Glycine During Crystallization from Solution

To illustrate the application of the in situ solid-state NMR technique, we focus on studies of the crystallization of glycine [ $\text{H}_2\text{C}(\text{NH}_3^+)(\text{CO}_2^-)$ ] from different solvents. Under ambient conditions, three polymorphs of glycine (denoted a, b, and g) are known.<sup>[67–71]</sup> The thermodynamically stable form is the g polymorph, and the least stable form is the b polymorph.<sup>[72, 73]</sup> According to the literature, crystallization of glycine from water at neutral pH produces the metastable a polymorph. However, a paper published in 1961 suggested<sup>[69]</sup> that crystallization of glycine from deuterated water may promote the formation of the g polymorph, although systematic studies of this isotope effect were only reported recently,<sup>[74, 75]</sup> in which it was demonstrated inter alia that deuteration (even as low as 1 % deuteration) does significantly increase the probability of obtaining the g polymorph. In high-resolution solid-state  $^{13}\text{C}$  NMR spectra, the isotropic  $^{13}\text{C}$  chemical shifts for the carboxylate carbon environment in the a, b, and g polymorphs of glycine are 176.5, 175.5, and 174.5 ppm respectively,<sup>[76]</sup> allowing the three polymorphs to be readily distinguished.

In the in situ  $^{13}\text{C}$  NMR study<sup>[62]</sup> of the crystallization of glycine (for a sample  $^{13}\text{C}$ -labelled in both carbon sites in the molecule) from water with natural isotopic abundance (Figure 13a), a peak emerges at 176.5 ppm and the intensity increases as a function of time. From the  $^{13}\text{C}$  chemical shift, this solid phase is assigned as the a polymorph. Thus, formation and growth of the a polymorph is observed, consistent with the literature, and no detectable amounts of the b or g polymorphs are observed during the crystallization

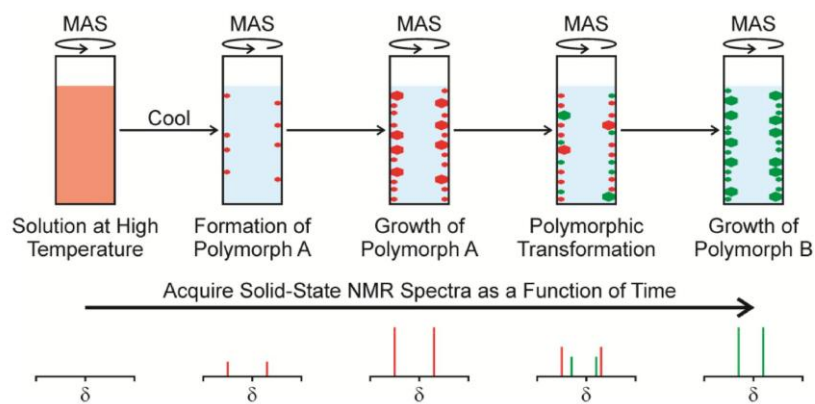


**Figure 12.** Schematic of the experimental strategy for in situ solid-state NMR studies of crystallization processes, illustrated for a system in which crystallization from solution initially produces a metastable polymorph A (red) followed by a polymorphic transformation to produce a more stable polymorph B (green). The corresponding changes in the high-resolution solid-state NMR spectrum, as a function of time, are shown at the bottom.

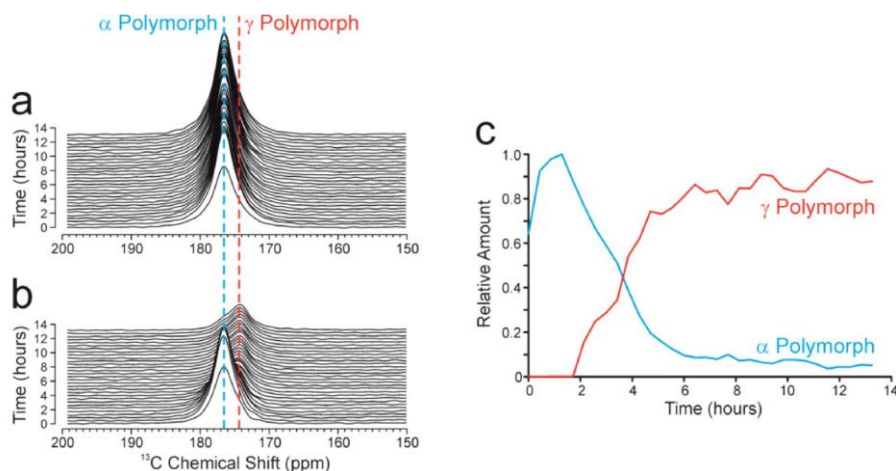


**Figure 13.** In situ solid-state  $^{13}\text{C}$  NMR spectra (showing only the carboxylate region) re-recorded as a function of time during crystal-lization of glycine from (a)  $\text{H}_2\text{O}$  and (b)  $\text{D}_2\text{O}$ .

(c) The relative amounts of the  $\alpha$  polymorph (blue) and  $\gamma$  polymorph (red) present, as a function of time, during crystallization from  $\text{D}_2\text{O}$ , established from the in situ solid-state  $^{13}\text{C}$  NMR data shown in (b).

experiment (which was carried out for a total time of 13 hr). We note that a comprehensive study of the crystallization of glycine from water<sup>[75]</sup> (involving ex situ characterization by powder X-ray diffraction) has shown that the initially formed  $\alpha$  polymorph eventually transforms to the thermodynamically stable  $\gamma$  polymorph after a period of time that is typically of the order of several days.

To explore the isotope effect discussed above, crystallization of glycine (for a sample  $^{13}\text{C}$ -labelled in both carbon sites in the molecule) from deuterated water was studied.<sup>[62]</sup> The total level of deuteration of all exchangeable hydrogen sites in the system (i. e., water molecules and  $\text{NH}_3^+$  groups of the zwitterionic glycine molecules) was 86 %. From the in situ solid-state  $^{13}\text{C}$  NMR results (Figure 13 b), it is clear that the  $\alpha$  polymorph is again the first solid form produced in the crystallization process, suggesting that the same nucleation pathway is followed in both  $\text{H}_2\text{O}$  and  $\text{D}_2\text{O}$ . The amount of the  $\alpha$  polymorph increases during the first 1.5 hr of the crystallization process. However, at this time, a new peak emerges at 174.5 ppm, characteristic of the  $\gamma$  polymorph. The intensity of this new peak then increases with time, while the intensity of the peak due to the  $\alpha$  polymorph decreases. The relative amounts of the  $\alpha$  and  $\gamma$  polymorphs present as a function of time, established from integrated peak intensities (corrected to allow for the different cross-polarization efficiencies of the  $\alpha$  and  $\gamma$  polymorphs), are shown in Figure 13 c. There is no evidence for any intermediate solid phase in the transformation from the  $\alpha$  polymorph to the  $\gamma$  polymorph, consistent with the rate of increase of the  $\gamma$  polymorph mirroring the rate of decrease of the  $\alpha$  polymorph (Figure 13 c). As discussed elsewhere,<sup>[62, 64]</sup> the transformation from the  $\alpha$  polymorph to the  $\gamma$  polymorph during the evolution of the crystallization process is assigned as a solution-mediated polymorphic transformation, rather than a direct solid-solid transition.

For each of the two isotopomeric systems, the final polymorph obtained at the end of the in situ solid-state  $^{13}\text{C}$  NMR study (i. e., the  $\alpha$  polymorph in the natural abundance system and the  $\gamma$  polymorph in the deuterated system) is consistent with the preferred polymorphic outcome

observed in conventional (ex situ) laboratory crystallization experiments<sup>[75]</sup> carried out under the same conditions and over the same total period of time.

Although a comprehensive understanding of the fascinating isotope effect in the crystallization of glycine from  $\text{D}_2\text{O}$  versus  $\text{H}_2\text{O}$  remains to be established, it is noteworthy that the way in which the crystal structures of the  $\alpha$  and  $\gamma$  polymorphs of glycine change upon deuteration is significantly different. Thus, it has been shown<sup>[74]</sup> that the unit cell volume of the  $\gamma$  polymorph decreases upon deuteration whereas the unit cell volume of the  $\alpha$  polymorph increases upon deuteration, which could signify that the energy difference between the stable  $\gamma$  polymorph and the metastable  $\alpha$  polymorph may actually be greater for the deuterated system. However, we refrain from advancing this tentative thought until a rigorous theoretical analysis has been carried out.

It is relevant to note that, as with most of the important topics in structural chemistry, Jack Dunitz has explored<sup>[77]</sup> the effects of deuteration on structural properties from the fundamental physicochemical viewpoint, and has applied his ideas in the case of crystalline benzene. In particular, this work demonstrated experimentally (from accurate neutron powder diffraction studies) and provided a fundamental rationalization of the fact that, below ca. 170 K, the volume per molecule in the crystal structure of deuterated benzene ( $\text{C}_6\text{D}_6$ ) is lower than the volume per molecule in the crystal structure of benzene with natural isotopic abundances ( $\text{C}_6\text{H}_6$ ), whereas above this temperature, the volume per molecule in the crystal structure of  $\text{C}_6\text{D}_6$  is higher than that of  $\text{C}_6\text{H}_6$ .

The results from an in situ solid-state  $^{13}\text{C}$  NMR study of the crystallization of glycine from methanol/water<sup>[63]</sup> are shown in Figure 14 (in this experiment, the glycine sample was  $^{13}\text{C}$ -labelled only in the carboxylate group, giving significantly narrower peaks than those in Figures 13 a and 13 b). In the first spectrum recorded, the solid phase is identified as a virtually pure sample of the  $\beta$  polymorph (a very small amount of the  $\alpha$  polymorph is also present). Thus, the very early stages of crystallization yield a significant excess of the  $\beta$  polymorph in this system. Subsequently, the  $\beta$

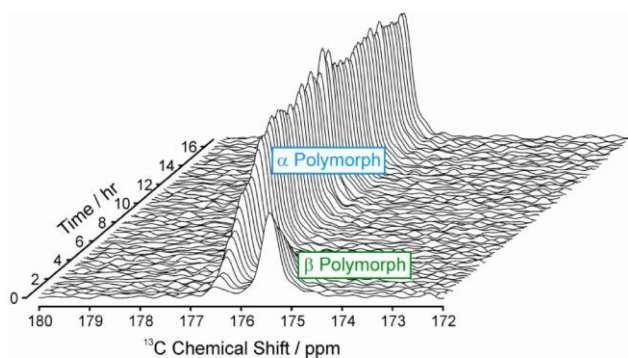


**Figure 14.** In situ solid-state  $^{13}\text{C}$  NMR spectra (showing the carboxylate region) recorded as a function of time during crystallization of glycine from methanol/water.

polymorph transforms to the  $\alpha$  polymorph by a solution-mediated transformation. Importantly, the results from our in situ solid-state  $^{13}\text{C}$  NMR study allow the timescale of the transformation from the  $\beta$  polymorph to the  $\alpha$  polymorph to be established, and indicate that a viable strategy for isolating the  $\beta$  polymorph would be to stop the crystallization experiment at the stage of the initial crystallization product, within only a few minutes of triggering the crystallization process.

#### 4.4 Combined Solid-state and Liquid-state NMR Studies of Crystallization Processes

A recent development<sup>[66]</sup> of the in situ NMR technique, with the potential to yield significantly deeper insights into crystallization processes than the version described above, exploits the fact that NMR can study both the liquid phase and the solid phase in a heterogeneous solid/liquid system using the same instrument, simply by changing the pulse sequence used to record the NMR data. Specifically, by alternating between two different pulse sequences in an in situ NMR study of crystallization, alternate solid-state NMR spectra and liquid-state NMR spectra are recorded, yielding essentially simultaneous information on the time evolution of both the solid phase and the liquid phase during the crystallization process. This strategy is called “CLASSIC NMR” (combined liquid- and solid-state in situ crystallization NMR). The CLASSIC NMR experiment creates the opportunity to elucidate the complementary changes that occur in the solid phase and in the liquid phase as a function of time during crystallization from solution. During the crystallization process, the changes in the amount and the identity of the solid phase are established from the time evolution of the solid-state NMR spectrum. Concomitantly, the solution phase becomes more dilute as the solid material is formed, and changes in the solution-state speciation and modes of molecular aggregation in solution are monitored from the time evolution of the liquid-state NMR spectrum.

In the case of the crystallization of m-aminobenzoic acid (m-ABA) from DMSO,<sup>[66]</sup> the simultaneous use of both solid-state NMR and liquid-state NMR to probe the crystallization process has revealed significant insights (from the liquid-state data) into the nature of the supersaturated solution that exists prior to nucleation, in comparison with the equilibrium saturated solution that exists at the end of the crystallization process. In particular, in comparison with the final equilibrium saturated solution, the prenucleation supersaturated solution contains a significantly higher proportion of zwitterionic m-ABA molecules and/or a significantly higher proportion of nonzwitterionic m-ABA molecules, in which the amino group acts as a hydrogen-bond acceptor (e. g., in hydrogen-bonded clusters of m-ABA molecules). As the solid form produced in crystallization of m-ABA from DMSO is the zwitterionic polymorph I, it is clear that the existence in solution of zwitterionic m-ABA molecules and/or prenucleation clusters of nonzwitterionic m-ABA molecules engaged in intermolecular  $\text{H}_2\text{N}\cdots\text{H}$  hydrogen bonding are very plausible precursors on the pathway to crystallization.

Clearly, the CLASSIC NMR experiment significantly extends the scope and capability of in situ monitoring of crystallization processes, as it is unique in providing simultaneous and complementary information on the time evolution of both the solid phase and the liquid phase. We fully anticipate that the advantages of the CLASSIC NMR strategy will yield significant new insights on a wide range of crystallization systems in the future.

#### 4.5 Some Fundamental Considerations

##### 4.5.1 What is the Smallest Size of Solid Particle that can be Detected in In Situ Solid-state NMR Studies of Crystallization?

An important question relates to the smallest size of solid particle that can be observed using the in situ NMR techniques described above, with implications on the earliest stage of the crystallization process that can be detected. As a basis for estimating the size limit,<sup>[64]</sup> we recall (Section 4.2) that selective detection of the NMR spectrum only of the solid phase is achieved using the  $^1\text{H}/^{13}\text{C}$  cross-polarization (CP) technique. The key limitation for obtaining a signal by CP is the rate of tumbling of the solid particle, as this motion “scrambles” the orientation of the dipolar couplings responsible for the polarization transfer. The tumbling motion is characterized by a correlation time ( $t_c$ ) which is related to the volume ( $V$ ) of the particle, the viscosity ( $\eta$ ) of the solvent, and the temperature ( $T$ ), through the Stokes-Einstein-Debye relation:<sup>[78]</sup>

$$t_c = \frac{6 V \eta}{k_B T l(l+1) \rho} ,$$

where  $l$  is the order of the spherical harmonic for the



interaction ( $l=2$  for dipolar coupling). Nowacka et al.<sup>[79]</sup> established that, for a  $^1\text{H}/^{13}\text{C}$  CP experiment to give a signal under similar conditions to those used in our experiments, the limiting value of  $t_c$  is ca. 10 ms. Using the above equation and taking the bulk viscosity of water (ca.  $10^{-3}$  Pa s), the limiting volume is estimated to be  $V = 4 \times 10^{-7} \text{ Å}^3$ , corresponding to a sphere with radius of ca. 210 Å. To put this value in context, particles of glycine of this size would contain around  $5 \times 10^5$  molecules. Although some approximations are inherent in this derivation, it nevertheless offers a reasonable estimate of the smallest size of solid particle that could be detected in an in situ solid-state NMR study of crystallization. Although the size of the critical nucleation entity may vary significantly between different systems and under different experimental conditions, the critical nucleation clusters for organic crystals are expected to comprise significantly less than  $5 \times 10^5$  molecules. Thus, the smallest solid particles that can be observed under the conditions of in situ solid-state NMR studies using the  $^1\text{H}/^{13}\text{C}$  CP technique are likely to represent postnucleation stages of the crystallization process. We note that, after observing the first peaks for the solid phase in our in situ solid-state NMR studies of crystallization processes using the  $^1\text{H}/^{13}\text{C}$  CP technique, we do not observe any evolution of the isotropic chemical shifts nor any evolution in the peak widths as a function of time, which is consistent with our conclusion that a signal is observed only for solid particles that are sufficiently large to behave as the “bulk” solid.

#### 4.5.2 Does the NMR Measurement Technique Itself Influence the Crystallization Process?

Another important question is whether the rapid sample rotation (MAS) required to record high-resolution solid-state NMR spectra may actually influence the pathway and/or the final outcome of the crystallization process, recognizing that rapid sample spinning exerts a centrifugal pressure on the sample. The pressure distribution within a sample subjected to spinning in a cylindrical rotor is readily calculated if the density distribution is known. Under typical conditions used in in situ solid-state NMR experiments to study crystallization processes, the induced pressure is estimated<sup>[64]</sup> to be in the region of 50–70 atm. As such pressures are significantly lower than those typically required to induce transformations to produce “high-pressure” polymorphs of organic materials, it is unlikely that the pressure generated by MAS will induce polymorphic transitions directly within the solid phase, except in very rare cases.

However, it is more important to consider the effects of the pressure induced by MAS on the solution phase properties of the crystallization system. First, it is important to recognize that rapid sample spinning induces a pressure gradient across the cylindrical sample volume. The induced pressure is zero on the rotation axis of the NMR rotor and increases radially towards the walls of the rotor. In the case of a homogeneous solution inside the rotor prior to crystallization, the solution

must respond to such a pressure gradient by redistribution of mass towards the outer part of the rotor, creating a density gradient across the sample (with lowest density at the centre of the rotor and highest density at the walls). The existence of such a density gradient may have important implications for the ensuing crystallization process, particularly as it implies that there may be a nonuniform distribution of concentration across the solution. Furthermore, as solubility is a function of pressure, the solubility may be different in different regions of the sample. Clearly, the confluence of these factors may create a significantly more complex crystallization environment than that encountered in conventional laboratory crystallization experiments. In our experience, however, we have not yet observed any systems for which the final solid form extracted from the NMR rotor following an in situ crystallization study differs from the final solid form resulting from crystallization in the laboratory under the same conditions and carried out over a comparable period of time. However, we cannot rule out the possibility that the effects of rapid sample spinning may influence the pathway and outcome of the crystallization process in some specific cases. We are currently embarking on a programme of research to investigate the effects of rapid sample spinning on solution behaviour from a deeper physicochemical perspective.

Finally, we note that a previous study<sup>[80]</sup> observed that the polymorphic outcome of a solid-state dehydration process may be influenced by the effects of rapid sample spinning in a solid-state NMR experiment. For in situ solid-state NMR studies of dehydration of sodium acetate trihydrate, the dehydration process was found to produce a different distribution of the polymorphs of anhydrous sodium acetate when dehydration was carried out under conditions of rapid sample spinning (leading to a mixture of polymorph I and polymorph beta of anhydrous sodium acetate) compared with dehydration of a static (nonspinning) sample under normal laboratory conditions (leading to the formation of only polymorph beta of anhydrous sodium acetate).

## 5. Future Challenges

As mentioned in Section 1, I believe that the most significant and important challenge in structural chemistry in the next few decades will be to derive a fundamental physicochemical understanding of the process of crystal nucleation, and then, based on this understanding, to devise experimental strategies to enable crystallization processes to be controlled such that they are directed towards very specific desired outcomes.

At present, a fashionable area of research is the computational prediction of all energetically reasonable crystal structures for a given organic molecule.<sup>[81–85]</sup> In many respects, however, the results of such “crystal structure prediction” calculations, which assess the energies of a large number of computer-generated crystal structures, produce more questions than answers. Perhaps the most significant issue is that crystal structure prediction calculations typically generate a vast

number (perhaps even hundreds) of distinct crystal structures within an energetically accessible range of the lowest-energy structure, implying that all of these structures may be viable as experimentally observable polymorphs. In the experimental context, however, it is rare for an organic compound to exhibit

more than three or four known polymorphic forms, while many organic compounds have only one experimentally known crystal structure. So, why do crystal structure prediction calculations generate so many plausible polymorphic forms, yet Nature appears to allow only a very small subset of these polymorphs to arise in practice? Is this situation a consequence of deficiencies in the computational techniques? Or is it simply that not enough experiments have been done under different crystallization conditions to allow all the energetically accessible polymorphs to be found? Or is it the case that many of the “unobserved” polymorphs are actually produced during crystallization, but have a very facile pathway to form a more stable polymorph (i. e., low barriers to transformation on the energy landscape) and therefore have only transitory existence during crystallization experiments (perhaps with significantly shorter lifetimes than the transient polymorphs revealed by the in situ solid-state NMR studies discussed in Section 4.3)? Or, instead, does Nature impose stringent rules governing crystallization pathways, such that feasible pathways exist only for a very limited subset of the energetically accessible bulk crystal structures predicted in the calculations? While all of these possibilities may contribute to the disparity between the computational predictions and experimental reality, it is most likely that the disparity is a consequence of our lack of understanding of the fundamental factors that underlie crystallization processes, and in particular our lack of detailed physicochemical knowledge of the critical events that constitute crystal nucleation.

At present, we have a reasonably good understanding of the nature of solution phases and the types of molecular aggregation that may occur to form small molecular clusters (for example, from solution-state NMR<sup>[86]</sup> or computer-simulation<sup>[87]</sup> studies) of the type that might represent the very earliest stages on the pathway towards crystallization. And we already have a comprehensive understanding of the structural properties and physical properties of the final “bulk” crystalline materials that represent the endpoints of crystallization processes (from the extensive range of powerful diffraction-based and spectroscopic techniques, some of which have been discussed in earlier sections of this article). However, the significant challenge is to fill the huge “knowledge void” that exists between the earliest stages and the final stage of the crystallization pathway. In particular, it is imperative to be able to identify and understand the critical events that give rise to crystal nucleation (representing the energy barrier that must be surmounted for crystal growth to occur), and to unravel the physicochemical factors that control crystal nucleation. Given that our understanding of crystal nucleation is based, to a large extent, on interpolating between our knowledge of the initial stages and the final stage of the crystallization pathway, it is not surprising that a number of different approaches for

rationalizing crystal nucleation have been proposed and are still actively debated.<sup>[88–92]</sup>

Experimental studies to observe and identify the critical nucleation events in crystallization processes are challenging for several reasons: 1) nucleation events are rare; 2) given that critical nucleation entities are species of high energy on the crystallization pathway, the population of such species is inevitably low and the lifetime of such species is inevitably short; 3) critical nucleation entities are likely to be in a size regime that is inaccessible to most techniques for structural analysis (i. e., significantly larger than small molecular clusters of the type that may be observed and structurally identified by traditional solution-state techniques, and significantly smaller than the size of crystalline aggregates that may be observed and structurally identified by traditional bulk solid-state techniques), and 4) even if the sizes of critical nucleation entities are accessible to experimental observation, it is likely that, within the crystallization solution, there will be a much higher population of (lower-energy) prenucleation entities and/or a much higher population of (lower-energy) postnucleation entities, such that to identify the critical nucleation entities from among the mixture of particles of different sizes (each representing a different point along the crystallization trajectory) may be exceptionally difficult. Given these issues, the current prospects for mapping the complete crystallization pathway by experimental observation, including identification of the critical events that correspond to crystal nucleation, are inherently very challenging. Nevertheless, small but significant steps of progress are being made by exploiting high-resolution imaging techniques,<sup>[93–95]</sup> in which clusters of the type that may be important in nucleation are observed either by direct in situ studies of the crystallization system (for example, by liquid-phase transmission electron microscopy (TEM) or in situ AFM) or through indirect ex situ studies (for example, by rapid freezing of samples extracted from the crystallization system followed by characterization using cryo-TEM techniques). We note that, for certain systems, there may also be opportunities to develop strategies to gain insights into the embryonic stages of crystal growth processes by retro-spective analysis of fully formed crystals recovered at the end of the crystallization process.<sup>[96]</sup>

From our present perspective and projecting into the future, perhaps the most promising opportunity to observe a system on the pathway towards nucleation and beyond, and hence implicitly to identify the critical nucleation events, will be to exploit computer-simulation techniques. One technical challenge in this endeavour, however, is that ideally the computer simulation should consider a system comprising a sufficiently large number of molecules (to enable a reasonably sized fragment of bulk crystal to be grown by the end of the simulation) and should be run over a sufficiently long period of time (to have a reasonable chance of observing an event as rare as nucleation, and then to be able to follow the growth of the fragment of bulk crystal beyond the nucleation event). In the favourable case that a nucleation event does indeed occur during the simulation, this approach will yield critical insights

into the structural changes (and the corresponding energetic changes) that occur along the crystallization pathway, yielding exquisite detail of the structural evolution towards nucleation, and mechanistic details of the nucleation event itself.

Fortunately, recent progress towards the application of computer-simulation methodologies to observe and understand mechanistic aspects of crystal nucleation appears promising.<sup>[97–102]</sup> Thus, as we look towards the horizon of present capabilities and contemplate the range of fundamental insights that we wish to discover, the prospects for exploiting computer-simulation techniques to unravel the intricate and complex details of crystallization pathways appear to provide the most optimistic opportunities. And then, looking even further into the future, once a sufficient level of fundamental understanding of the physicochemical factors that control crystal nucleation have been established, we will be in a favourable position to exploit this understanding in formulating strategies to control crystallization pathways towards achieving specific desired outcomes.

## Acknowledgements

I am very grateful to many students, postdoctoral researchers, and collaborators, past and present, who have contributed to the research described in this article. Dr. Colan Hughes is thanked for help in checking the manuscript.

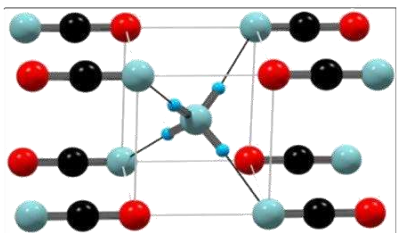
## References

- [1] J. D. Dunitz, *X-ray Analysis and the Structure of Organic Molecules*, Cornell University Press, Ithaca, 1979.
- [2] K. N. Trueblood, J. D. Dunitz, *Acta Crystallogr. Sect. B: Struct. Sci.* 1983, 39, 120.
- [3] J. D. Dunitz, V. Schomaker, K. N. Trueblood, *J. Phys. Chem.* 1988, 92, 856.
- [4] J. D. Dunitz, E. F. Maverick, K. N. Trueblood, *Angew. Chemie Int. Ed. Engl.* 1988, 27, 880.
- [5] J. D. Dunitz, *Pure Appl. Chem.* 1991, 63, 177.
- [6] J. D. Dunitz, J. Bernstein, *Acc. Chem. Res.* 1995, 28, 193.
- [7] J. D. Dunitz, *Acta Crystallogr. Sect. B: Struct. Sci.* 1995, 51, 619.
- [8] K. D. M. Harris, *Top. Curr. Chem.* 2012, 315, 133.
- [9] B. A. Palmer, G. R. Edwards-Gau, B. M. Kariuki, K. D. M. Harris, I. P. Dolbnya, S. P. Collins, *Science* 2014, 344, 1013.
- [10] J. M. Thomas, *Isr. J. Chem.* 2017, DOI: 10.1002/ijch.201600053.
- [11] D. C. Apperley, R. K. Harris, P. Hodgkinson, *Solid State NMR: Basic Principles & Practice*, Momentum Press LLC, New York, 2012.
- [12] M. J. Duer, *Introduction to Solid-State NMR Spectroscopy*, Blackwell Publishing Ltd, Oxford, 2004.
- [13] J. Seelig, *Q. Rev. Biophys.* 1977, 10, 353.
- [14] L. W. Jelinski, *Ann. Rev. Mater. Sci.* 1985, 15, 359.
- [15] R. R. Vold, R. L. Vold, *Adv. Magn. Opt. Reson.* 1991, 16, 85.
- [16] G. L. Hoatson, R. L. Vold, *NMR* 1994, 32, 3.
- [17] A. E. Aliev, K. D. M. Harris, *Struct. Bonding* 2004, 108, 1.
- [18] R. W. G. Wyckoff, R. B. Corey, *Z. Kristallogr. Kristallgeom. Kristallphys. Kristallchem.* 1934, 89, 462.
- [19] P. Vaughan, J. Donohue, *Acta Crystallogr.* 1952, 5, 530.
- [20] P. Vaughan, J. Donohue, *Acta Crystallogr. Sect. B: Struct. Crystallogr. Cryst. Chem.* 1969, 25, 404.
- [21] J. W. Emsley, J. A. S. Smith, *Trans. Faraday Soc.* 1961, 57, 1233.
- [22] T. Chiba, *Bull. Chem. Soc. Japan* 1965, 38, 259.
- [23] A. Zussman, *J. Chem. Phys.* 1973, 58, 1514.
- [24] A. E. Aliev, S. P. Smart, K. D. M. Harris, *J. Mater. Chem.* 1994, 4, 35.
- [25] S. J. Kitchin, S. Ahn, K. D. M. Harris, *J. Phys. Chem. A* 2002, 106, 7228.
- [26] M. S. Lehmann, A. C. Nunes, *Acta Crystallogr. Sect. B: Struct. Crystallogr. Cryst. Chem.* 1980, 36, 1621.
- [27] M. S. Lehmann, T. F. Koetzle, W. C. Hamilton, *J. Cryst. Mol. Struct.* 1972, 2, 225.
- [28] J. D. Dunitz, A. Gavezzotti, *J. Phys. Chem. B* 2012, 116, 6740.
- [29] S. J. Kitchin, G. Tutoveanu, M. R. Steele, E. L. Porter, K. D. M. Harris, *J. Phys. Chem. B* 2005, 109, 22808.
- [30] J. R. Long, B. Q. Sun, A. Bowen, R. G. Griffin, *J. Am. Chem. Soc.* 1994, 116, 11950.
- [31] Z. T. Gu, K. Ebisawa, A. McDermott, *Solid State Nucl. Magn. Reson.* 1996, 7, 161.
- [32] A. E. Aliev, S. E. Mann, A. S. Rahman, P. F. McMillan, F. Corà, D. Iuga, C. E. Hughes, K. D. M. Harris, *J. Phys. Chem. A* 2011, 115, 12201.
- [33] G. Ferguson, J. F. Gallagher, C. Glidewell, J. N. Low, S. N. Scrimgeour, *Acta Crystallogr. Sect. C: Cryst. Struct. Commun.* 1992, 48, 1272.
- [34] A. E. Aliev, E. J. MacLean, K. D. M. Harris, B. M. Kariuki, C. Glidewell, *J. Phys. Chem. B* 1998, 102, 2165.
- [35] H. Serrano-González, K. D. M. Harris, C. C. Wilson, A. E. Aliev, S. J. Kitchin, B. M. Kariuki, M. Bach-Vergés, C. Glidewell, E. J. MacLean, W. W. Kagunya, *J. Phys. Chem. B* 1999, 103, 6215.
- [36] A. E. Aliev, C. E. Atkinson, K. D. M. Harris, *J. Phys. Chem. B* 2002, 106, 9013.
- [37] M. Mella, K. D. M. Harris, *Phys. Chem. Chem. Phys.* 2009, 11, 11340.
- [38] J. Kärger, D. M. Ruthven, *Diffusion in Zeolites and Other Microporous Solids*, John Wiley & Sons, New York, 1992.
- [39] H. Jobic, D. N. Theodorou, *Microporous Mesoporous Mater.* 2007, 102, 21.
- [40] A. A. Khan, S. T. Bramwell, K. D. M. Harris, B. M. Kariuki, M. R. Truter, *Chem. Phys. Lett.* 1999, 307, 320.
- [41] A. E. Smith, *Acta Crystallogr.* 1952, 5, 224.
- [42] K. D. M. Harris, J. M. Thomas, *J. Chem. Soc. Faraday Trans.* 1990, 86, 2985.
- [43] M. D. Hollingsworth, K. D. M. Harris, in *Comprehensive Supramolecular Chemistry* (Eds.: D. D. MacNicol, F. Toda, R. Bishop), Pergamon, 1996, Volume 6, pp. 177–237.
- [44] K. D. M. Harris, *Chem. Soc. Rev.* 1997, 26, 279.
- [45] K. D. M. Harris, *Supramol. Chem.* 2007, 19, 47.
- [46] J. Martí-Rujas, A. Desmedt, K. D. M. Harris, F. Guillaume, *J. Am. Chem. Soc.* 2004, 126, 11124.
- [47] J. Martí-Rujas, A. Desmedt, K. D. M. Harris, F. Guillaume, *J. Phys. Chem. B* 2007, 111, 12339.
- [48] J. Martí-Rujas, K. D. M. Harris, A. Desmedt, F. Guillaume, *J. Phys. Chem. B* 2006, 110, 10708.
- [49] J. Martí-Rujas, A. Desmedt, K. D. M. Harris, F. Guillaume, *J. Phys. Chem. C* 2009, 113, 736.
- [50] F. Wöhler, *Ann. Phys. Chem.* 1828, 12, 253.
- [51] J. Liebig, F. Wöhler, *Ann. Phys. Chem.* 1830, 20, 369.



- [52] J. Shorter, *Chem. Soc. Rev.* 1978, 77, 21.
- [53] J. D. Dunitz, K. D. M. Harris, R. L. Johnston, B. M. Kariuki, E. J. MacLean, K. Psallidas, W. B. Schweizer, R. R. Tykwinski, *J. Am. Chem. Soc.* 1998, 120, 13274.
- [54] E. J. MacLean, K. D. M. Harris, B. M. Kariuki, S. J. Kitchin, R. R. Tykwinski, I. P. Swainson, J. D. Dunitz, *J. Am. Chem. Soc.* 2003, 125, 14449.
- [55] A. Desmedt, S. J. Kitchin, K. D. M. Harris, F. Guillaume, R. R. Tykwinski, M. Xu, M. A. Gonzalez, *J. Phys. Chem. C* 2008, 112, 15870.
- [56] A. Alavi, R. J. C. Brown, S. Habershon, K. D. M. Harris, R. L. Johnston, *Mol. Phys.* 2004, 102, 869.
- [57] T. M. Alam, G. P. Drobny, *Chem. Rev.* 1991, 91, 1545.
- [58] C. A. Tsipis, P. A. Karipidis, *J. Am. Chem. Soc.* 2003, 125, 2307.
- [59] R. Méreau, A. Desmedt, K. D. M. Harris, *J. Phys. Chem. B* 2007, 111, 3960.
- [60] N. Pienack, W. Bensch, *Angew. Chem. Int. Ed.* 2011, 50, 2014.
- [61] K. D. M. Harris, C. E. Hughes, P. A. Williams, *Solid State Nucl. Magn. Reson.* 2015, 65, 107.
- [62] C. E. Hughes, K. D. M. Harris, *J. Phys. Chem. A* 2008, 112, 6808.
- [63] C. E. Hughes, K. D. M. Harris, *Chem. Commun.* 2010, 46, 4982.
- [64] C. E. Hughes, P. A. Williams, V. L. Keast, V. G. Charalampo-poulos, G. R. Edwards-Gau, K. D. M. Harris, *Faraday Discuss.* 2015, 179, 115.
- [65] C. E. Hughes, P. A. Williams, T. R. Peskett, K. D. M. Harris, *J. Phys. Chem. Lett.* 2012, 3, 3176.
- [66] C. E. Hughes, P. A. Williams, K. D. M. Harris, *Angew. Chemie Int. Ed.* 2014, 53, 8939.
- [67] G. Albrecht, R. B. Corey, *J. Am. Chem. Soc.* 1939, 61, 1087.
- [68] Y. Iitaka, *Acta Crystallogr.* 1960, 13, 35.
- [69] Y. Iitaka, *Acta Crystallogr.* 1961, 14, 1.
- [70] P.-G. Jönsson, Å. Kvik, *Acta Crystallogr. Sect. B: Struct. Crystallogr. Cryst. Chem.* 1972, 28, 1827.
- [71] Å. Kvik, W. M. Canning, T. F. Koetzle, G. J. B. Williams, *Acta Crystallogr. Sect. B: Struct. Crystallogr. Cryst. Chem.* 1980, 36, 115.
- [72] E. V. Boldyreva, V. A. Drebuschak, T. N. Drebuschak, I. E. Paukov, Y. A. Kovalevskaya, E. S. Shutova, *J. Therm. Anal. Calorim.* 2003, 73, 409.
- [73] G. L. Perlovich, L. K. Hansen, A. Bauer-Brandl, *J. Therm. Anal. Calorim.* 2001, 66, 699.
- [74] C. E. Hughes, S. Hamad, K. D. M. Harris, C. R. A. Catlow, P. C. Griffiths, *Faraday Discuss.* 2007, 136, 71.
- [75] C. E. Hughes, K. D. M. Harris, *New J. Chem.* 2009, 33, 713.
- [76] R. E. Taylor, *Concepts Magn. Reson. Part A* 2004, 22 A, 79.
- [77] J. D. Dunitz, R. M. Ibberson, *Angew. Chemie Int. Ed.* 2008, 47, 4208.
- [78] P. Debye, *Polar Molecules*, The Chemical Catalog Company, New York, 1929.
- [79] A. Nowacka, P. C. Mohr, J. Norrman, R. W. Martin, D. Topgaard, *Langmuir* 2010, 26, 16848.
- [80] M. Xu, K. D. M. Harris, *J. Am. Chem. Soc.* 2005, 127, 10832.
- [81] A. Gavezzotti, *Acc. Chem. Res.* 1994, 27, 309.
- [82] A. R. Oganov, C. W. Glass, *J. Chem. Phys.* 2006, 124, 244704.
- [83] G. M. Day, *Crystallogr. Rev.* 2011, 17, 3.
- [84] S. L. Price, *Acta Crystallogr. Sect. B: Struct. Sci. Cryst. Eng. Mater.* 2013, 69, 313.
- [85] S. L. Price, *Chem. Soc. Rev.* 2014, 43, 2098.
- [86] A. Spitaleri, C. A. Hunter, J. F. McCabe, M. J. Packer, S. L. Cockcroft, *CrystEngComm* 2004, 4, 489.
- [87] S. Hamad, C. E. Hughes, C. R. A. Catlow, K. D. M. Harris, *J. Phys. Chem. B* 2008, 112, 7280.
- [88] D. Erdemir, A. Y. Lee, A. S. Myerson, *Acc. Chem. Res.* 2009, 42, 621.
- [89] R. J. Davey, S. L. M. Schroeder, J. H. ter Horst, *Angew. Chemie Int. Ed.* 2013, 52, 2166.
- [90] J. J. De Yoreo, P. U. P. A. Gilbert, N. A. J. M. Sommerdijk, R. L. Penn, S. Whitelam, D. Joester, H. Z. Zhang, J. D. Rimer, A. Navrotsky, J. F. Banfield, A. F. Wallace, F. M. Michel, F. C. Meldrum, H. Cölfen, P. M. Dove, *Science* 2015, 349, aaa6760.
- [91] D. Zahn, *ChemPhysChem* 2015, 16, 2069.
- [92] Nucleation – a Transition State to the Directed Assembly of Materials, *Faraday Discuss.* 2015, 179.
- [93] J. Baumgartner, A. Dey, P. H. H. Bomans, C. Le Coadou, P. Fratzl, N. A. J. M. Sommerdijk, D. Faivre, *Nat. Mater.* 2013, 12, 310.
- [94] W. J. E. M. Habraken, J. Tao, L. J. Brylka, H. Friedrich, L. Bertineti, A. S. Schenk, A. Verch, V. Dmitrovic, P. H. H. Bomans, P. M. Frederik, J. Laven, P. van der Schoot, B. Aichmayer, G. de With, J. J. De Yoreo, N. A. J. M. Sommerdijk, *Nat. Commun.* 2013, 4, 1507.
- [95] P. J. M. Smeets, K. R. Cho, R. G. E. Kempen, N. A. J. M. Sommerdijk, J. J. De Yoreo, *Nat. Mater.* 2015, 14, 394.
- [96] B. A. Palmer, K. D. M. Harris, F. Guillaume, *Angew. Chemie Int. Ed.* 2010, 49, 5096.
- [97] M. R. Walsh, C. A. Koh, E. D. Sloan, A. K. Sum, D. T. Wu, *Science* 2009, 326, 1095.
- [98] V. Agarwal, B. Peters, *Adv. Chem. Phys.* 2014, 155, 97.
- [99] D. Gebauer, M. Kellermeier, J. D. Gale, L. Bergström, H. Cölfen, *Chem. Soc. Rev.* 2014, 43, 2348.
- [100] F. Giberti, M. Salvalaglio, M. Parrinello, *IUCrJ* 2015, 2, 256.
- [101] Z. M. Aman, C. A. Koh, *Chem. Soc. Rev.* 2016, 45, 1678.
- [102] G. C. Sossio, J. Chen, S. J. Cox, M. Fitzner, P. Pedevilla, A. Zen, A. Michaelides, *Chem. Rev.* 2016, 116, 7078.

1  
2  
3  
4  
5  
6  
7  
8  
9  
10  
11  
12  
13  
14  
15  
16  
17  
18  
19  
20  
21  
22  
23  
24  
25  
26  
27  
28  
29  
30  
31  
32  
33  
34  
35  
36  
37  
38  
39  
40  
41  
42  
43  
44  
45  
46  
47  
48  
49  
50  
51  
52  
53  
54  
55  
56



K. D. M. Harris\*

1 – 18

Explorations in the Dynamics of  
Crystalline Solids and the Evolution  
of Crystal Formation Processes

